DOI: 10.2352/ISSN.2470-1173.2016.18.DPMI-256

Single-Sensor RGB and NIR Image Acquisition: Toward Optimal Performance by Taking Account of CFA Pattern, Demosaicking, and Colo

Hayato Teranaka, Yusuke Monno, Masayuki Tanaka and Masatoshi O
Department of Mechanical and Control Engineering, Tokyo Institute
2-12-1, O-okayama, Meguro-ku, Tokyo, Japan

Abstract

In recent years, many applications using a pair of RGB and near-infrared (NIR) images have been proposed in computer vision and image processing communities. Thanks to recent progress of image sensor technology, it is also becoming possible to manufacture an image sensor with a novel spectral filter array, which has RGB plus NIR pixels for one-shot acquisition of the RGB and the NIR images. In such a novel filter array, half of the G pixels in the standard Bayer color filter array (CFA) are typically replaced with the NIR pixels. However, its performance has not fully been investigated in the pipeline of single-sensor RGB and NIR image acquisition. In this paper, we present an imaging pipeline of the single-sensor RGB and NIR image acquisition and investigate its optimal performance by taking account of the filter array pattern, demosaicking and color correction. We also propose two types of filter array patterns and demosaicking algorithms for improving the quality of acquired RGB and NIR images. Based on the imaging pipeline we present, the performance of different filter array patterns and demosaicking algorithms is evaluated. In experimental results, we demonstrate that our proposed filter array patterns and demosaicking algorithms outperform the existing ones.

Introduction

In recent years, many applications using a pair of RGB and near-infrared (NIR) images have been proposed in computer vision and image processing communities such as image enhancement [1, 2], image fusion [3, 4], dehazing [5, 6], denoising [7, 8], and shadow detection [9]. However, the acquisition of the pair of RGB and NIR images is still a challenging task because existing acquisition systems typically require multiple cameras [1] or multiple shots [9], where one is required for RGB and the other is required for NIR.

In current compact and low-cost digital cameras, single-senor color image acquisition with the Bayer color filter array (CFA) [10], as shown in Fig. 1 (a)-(c), is well established [11]. To simultaneously acquire the RGB and the NIR images, many existing works extend the idea of using the CFA for single-sensor RGB and NIR image acquisition [12–18]. Thanks to recent progress of image sensor technology, it is also becoming possible to manufacture an image sensor with a novel filter array, which has RGB plus NIR pixels [14–18]. This sensor can provide us with a practical solution for one-shot acquisition of the RGB and the NIR images without increased size and cost from current color digital cameras. Hereafter, we call such a filter array "RGB-NIR filter array" and such a sensor "RGB-NIR sensor," respectively.

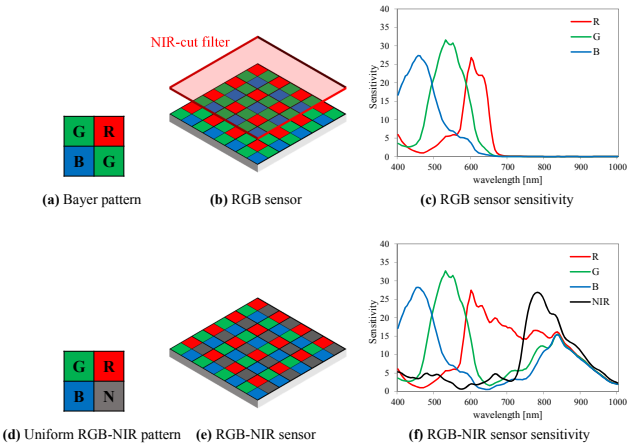

Figure 1: RGB sensor and RGB-NIR sensor: (a) Bayer pattern. (b) RGB sensor. (c) RGB sensor sensitivity. (d) Uniform RGB-NIR pattern. (e) RGB-NIR sensor. (f) RGB-NIR sensor sensitivity.

In the RGB-NIR filter array, half of the G pixels in the standard Bayer CFA are typically replaced with the NIR pixels [14–18], as shown in Fig. 1 (d)-(f). In other words, each spectral band is uniformly sampled in the filter array. We call this pattern "uniform RGB-NIR pattern" in this paper. In the single-sensor RGB and NIR image acquisition, the sensor output is mosaic data, where only one pixel value among R, G, B, and NIR values is recorded at each pixel location. Therefore, full RGB and NIR images need to be generated by an interpolation process, which is typically called demosaicking [19, 20]. Although it is known that both the filter array pattern and the demosaicking algorithm affect the quality of the acquired RGB and NIR images, the performance of the uniform RGB-NIR pattern has not fully been investigated in the past literatures [14–18].

The other challenge of the single-sensor RGB and NIR image acquisition is color correction. Since typical RGB filters have spectral sensitivities also in the NIR wavelengths (see Fig. 1 (f)), an NIR-cut filter is usually placed in front of the current RGB sensor to avoid NIR contaminations of the acquired RGB image (see Fig. 1 (b) and (c)). However, the NIR-cut filter needs to be removed to acquire both the RGB and the NIR images by the RGB-NIR sensor. Therefore, color correction is required for removing the NIR contaminations of the RGB image and reproducing the image with correct color representation [16, 21]. To investigate

DOI: 10.2352/ISSN.2470-1173.2016.18.DPMI-256

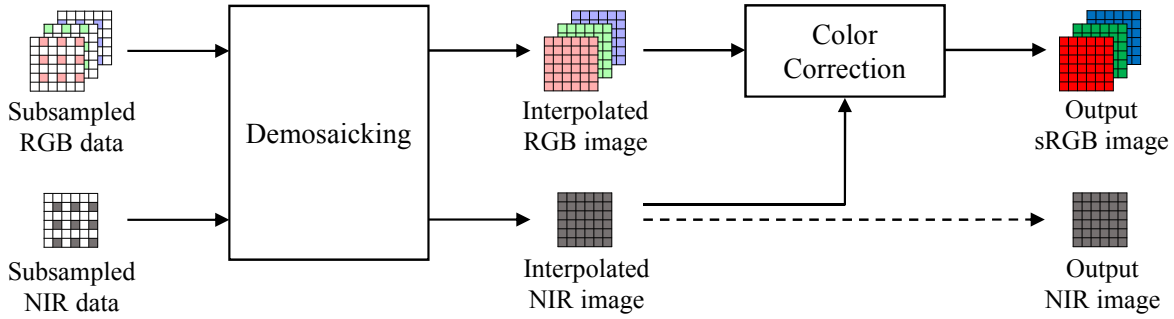

Figure 2: Image processing pipeline of the single-sensor RGB and NIR image acquisition.

an optimal performance of the single-sensor RGB and NIR image acquisition, it is important to take into account all of the filter array pattern, the demosaicking and the color correction, which has not fully been addressed in existing works.

In this paper, we first present an imaging pipeline of the single-sensor RGB and NIR image acquisition. Then, we investigate its optimal performance by taking account of the filter array pattern, the demosaicking and the color correction. Especially, we propose two types of filter array patterns and demosaicking algorithms for improving the quality of the acquired RGB and NIR images. Based on the imaging pipeline we present, the performance of different filter array patterns and demosaicking algorithms is evaluated in simulation experiments. In experimental results, we demonstrate that our proposed filter array patterns outperform the commonly used uniform pattern.

Imaging Processing Pipeline

Overview

Fig. 2 presents the standard image processing pipeline of the single-sensor RGB and NIR image acquisition. The pipeline consists of two successive image processing operations, demosaicking and color correction. The demosaicking is firstly performed to reconstruct full RGB and NIR images from the mosaicked sensor output, where only one spectral band is measured at each pixel location according to the filter array pattern. Then, color correction is performed for removing the NIR contaminations of the RGB image and reproducing the image with standard RGB (sRGB) representation [16, 21]. In the following, the detailed explanation of the filter array patterns, the demosaicking algorithms and the color correction is described. We also propose two novel filter array patterns for improving the performance of the single-sensor RGB and NIR image acquisition.

RGB-NIR Filter Array Patterns and Demosaicking Algorithms

Uniform RGB-NIR pattern. Fig. 3 (a) shows the uniform RGB-NIR pattern and its demosaicking flow by the state-of-the-art algorithm in [18]. The uniform RGB-NIR pattern is commonly used in existing works [14–18]. In the uniform RGB-NIR pattern, each spectral band is evenly sampled. In the demosaicking algorithm [18], the NIR band is firstly interpolated by bicubic interpolation. Then, the missing G pixel values at the NIR pixel locations are estimated by color difference interpolation to reconstruct the Bayer mosaic data. Finally, a Bayer demosaicking algorithm is performed to generate the interpolated RGB image. In experiments, we use the residual interpolation [22] for the Bayer demosaicking algorithm.

Proposed RGB-NIR pattern 1. Fig. 3 (b) shows the proposed RGB-NIR pattern 1 and its demosaicking flow. This pattern is an instance of the previously proposed pattern [23]. We design this pattern to have the following desirable properties: (i) The NIR pixels are sampled from the Bayer CFA, and (ii) the sampling density of the G pixels is as high as the Bayer CFA. In the same manner as most of the Bayer demosaicking algorithms, we first interpolate the missing G pixel values. The advantage of this pattern is that we can effectively generate a high-quality guide G image from the only subsampled RGB data, because the NIR pixels are sparsely sampled from the Bayer CFA. After generating the high-quality guide G image, we exploit inter-channel correlations to interpolate the missing R, B and NIR pixel values by residual interpolation [22]. We refer to the papers [22, 23] for detailed descriptions of the algorithm.

Proposed RGB-NIR pattern 2. Fig. 3 (c) shows the proposed RGB-NIR pattern 2 and its demosaicking flow. In common with the proposed RGB-NIR pattern 1, the proposed RGB-NIR pattern 2 also has the same sampling density of the G pixels as the Bayer CFA. However, the NIR pixels have a higher sampling density compared with the proposed RGB-NIR pattern 1. In the demosaicking algorithm, all of the R, G, B, and NIR bands are used for generating a high-quality guide G image. Then, we exploit inter-channel correlations to interpolate the missing R, B and NIR pixel values by residual interpolation [22]. We refer to the papers [22, 24] for detailed descriptions of the algorithm.

Color Correction

After generating the interpolated RGB and NIR images, color correction is performed to reproduce the sRGB image. We simply perform the linear mapping as

$$\begin{bmatrix} sR \\ sG \\ sB \end{bmatrix} = \begin{bmatrix} m_{11} & m_{12} & m_{13} & m_{14} \\ m_{21} & m_{22} & m_{23} & m_{24} \\ m_{31} & m_{32} & m_{33} & m_{34} \\ m_{41} & m_{42} & m_{43} & m_{44} \end{bmatrix} \begin{bmatrix} R \\ G \\ B \\ NIR \end{bmatrix}, \quad (1)$$

where $[sR, sG, sB]^T$ is a target sRGB vector and $[R, G, B, NIR]^T$ is a input intensity vector. The 3×4 color correction matrix is calculated by a least-square manner based on training samples.

DOI: 10.2352/ISSN.2470-1173.2016.18.DPMI-256

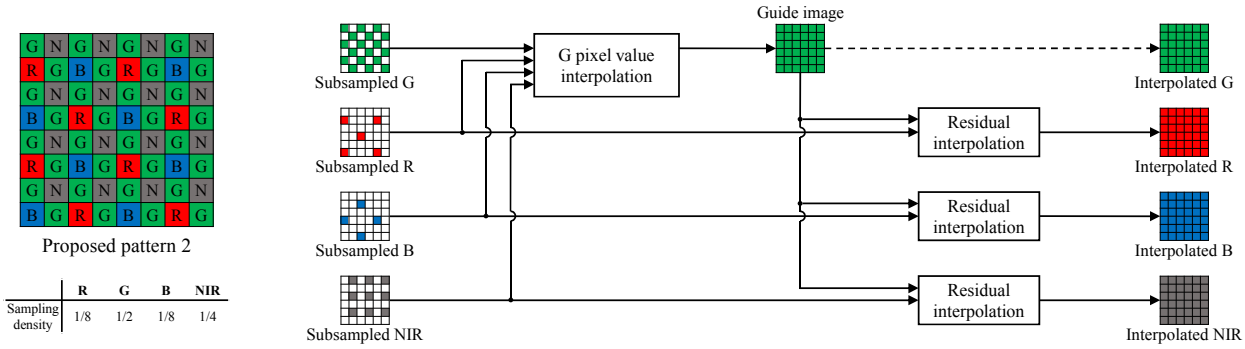

(c) Proposed RGB-NIR pattern 2 and its demosaicking flow.

Figure 3: Demosaicking flows with different RGB-NIR filter array patterns: (a) Uniform RGB-NIR pattern. (b) Proposed RGB-NIR pattern 1. (c) Proposed RGB-NIR pattern 2.

Experiments

In experiments, we used a hyperspectral image dataset including both visible and NIR wavelengths (420-1000nm). The hyperspectral image is acquired at every 10 nm by using a monochrome camera with two VariSpec tunable filters [25], VIS (420-640nm) and SNIR (650-1000nm). The captured hyperspectral image is then converted into a form of spectral reflectance using a calibration chart. In experimental evaluation, the whole imaging pipeline is simulated by using the hyperspectral dataset as the ground truth. The dataset consists of 40 scenes with 512×512 pixels, which is divided into two groups, where half 20 scenes are used for training the color correction matrix in Eq. (1) and the rest 20 scenes are used for testing the imaging pipeline. We assumed a daylight as a light source for the evaluation. Fig. 4 summarizes the pipeline of simulation experiments.

We compared three filter array patterns; (i) the uniform RGB-NIR pattern, (ii) the proposed RGB-NIR pattern 1, and (iii) the proposed RGB-NIR pattern 2. In the numerical comparison, we evaluate multispectral peak signal-to-noise ratio (MPSNR) calculated as

$$\mathrm{MPSNR} = 10\log \frac{255^2}{\frac{1}{4}\sum_{i=sR,sG,sB,NIR} ||\hat{x}_i - x_i||_2^2}, \qquad (2)$$

where $\hat{x}_i$ is the estimated pixel value and x_i is the ground-truth pixel value. Table 1 shows the MPSNR performance of the test 20 scenes. One can see that our proposed RGB-NIR patterns significantly outperform the uniform pattern. The proposed pattern 1 is slightly better than the proposed pattern 2. Fig. 5 shows the visual comparison of the acquired RGB and NIR images by different filter array patterns. From the visual comparison, our proposed RGB-NIR patterns can offer visually pleasing results, while the uniform RGB-NIR pattern generates severe visual artifacts in edges.

DOI: 10.2352/ISSN.2470-1173.2016.18.DPMI-256

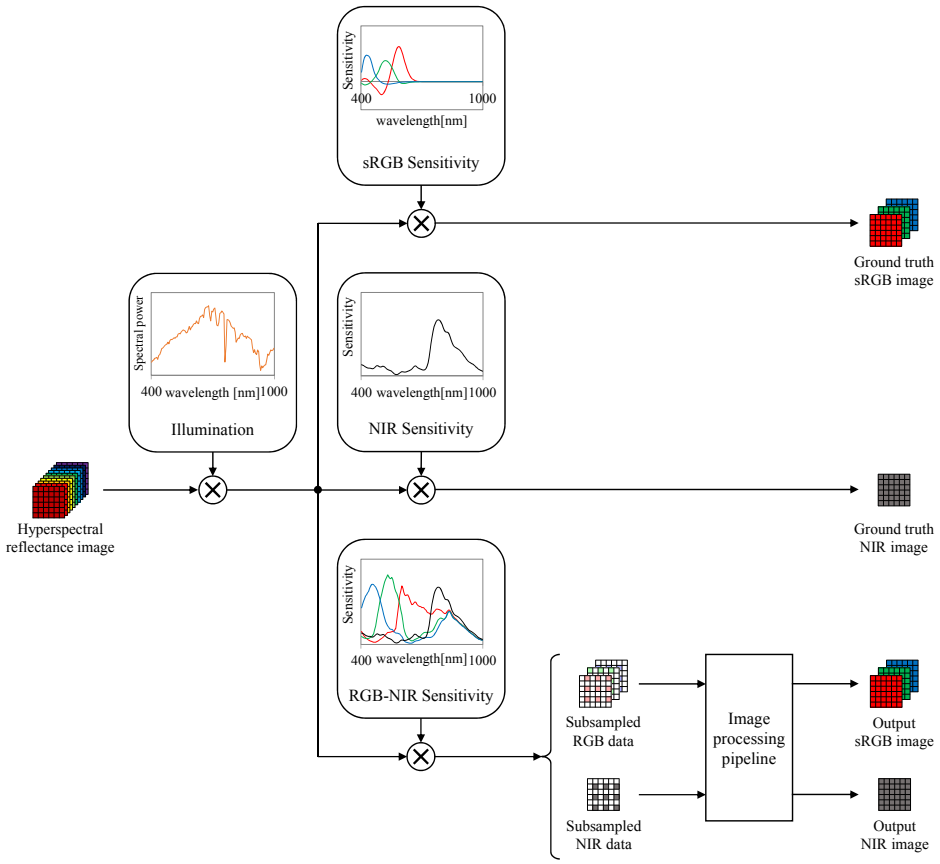

Figure 4: The pipeline of simulation experiments.

Conclusion

In this paper, we presented the image processing pipeline of the single-sensor RGB and NIR image acquisition and investigated its optimal performance by taking account of the filter array pattern, the demosaicking, and the color correction. We also proposed two novel filter array patterns and demosaicking algorithms to achieve a better performance for acquiring high-quality RGB and NIR images. The advantage of our proposed filter array patterns is that we keep the sampling density of the G pixels as high as the Bayer CFA. We experimentally compared the performance of the imaging pipeline with different filter array patterns and demonstrated that our proposed filter array patterns outperform the commonly used uniform pattern in terms of numerical and visual comparisons.

Acknowledgment

This work was partly supported by Strategic Information and Communications R&D Promotion Programme (SCOPE, No.141203024) from Ministry of Internal Affairs and Communications (MIC).

References

[1] X. Zhang, T. Sim, and X. Miao, "Enhancing photographs with near infra-red images," *Proc. of IEEE Conf. on Computer Vision and Pattern Recognition (CVPR)*, pp. 1–8, 2008.

[2] T. Shibata, M. Tanaka, and M. Okutomi, "Visible and near-infrared image fusion based on visually salient area selection," *Proc. of SPIE*,

Table 1: MPSNR performance for test 20 scenes.

#	Uniform	Proposed 1	Proposed 2
1	34.89	**38.53**	38.19
2	26.67	28.72	**29.47**
3	30.25	**34.06**	33.69
4	32.63	**36.16**	35.85
5	30.87	33.25	**33.26**
6	34.93	**36.18**	36.03
7	35.57	**37.97**	37.88
8	34.03	**34.73**	33.83
9	31.45	**35.17**	34.72
10	27.48	29.74	**29.95**
11	31.60	**33.26**	32.90
12	32.21	**35.89**	35.79
13	34.37	**35.11**	35.00
14	30.33	**31.41**	30.48
15	27.77	**29.72**	29.27
16	32.14	**36.55**	35.69
17	30.83	33.11	**33.62**
18	33.17	36.49	**36.77**
19	27.70	**34.07**	33.06
20	28.32	**29.63**	28.79
Ave.	31.36	**33.99**	33.71

DOI: 10.2352/ISSN.2470-1173.2016.18.DPMI-256

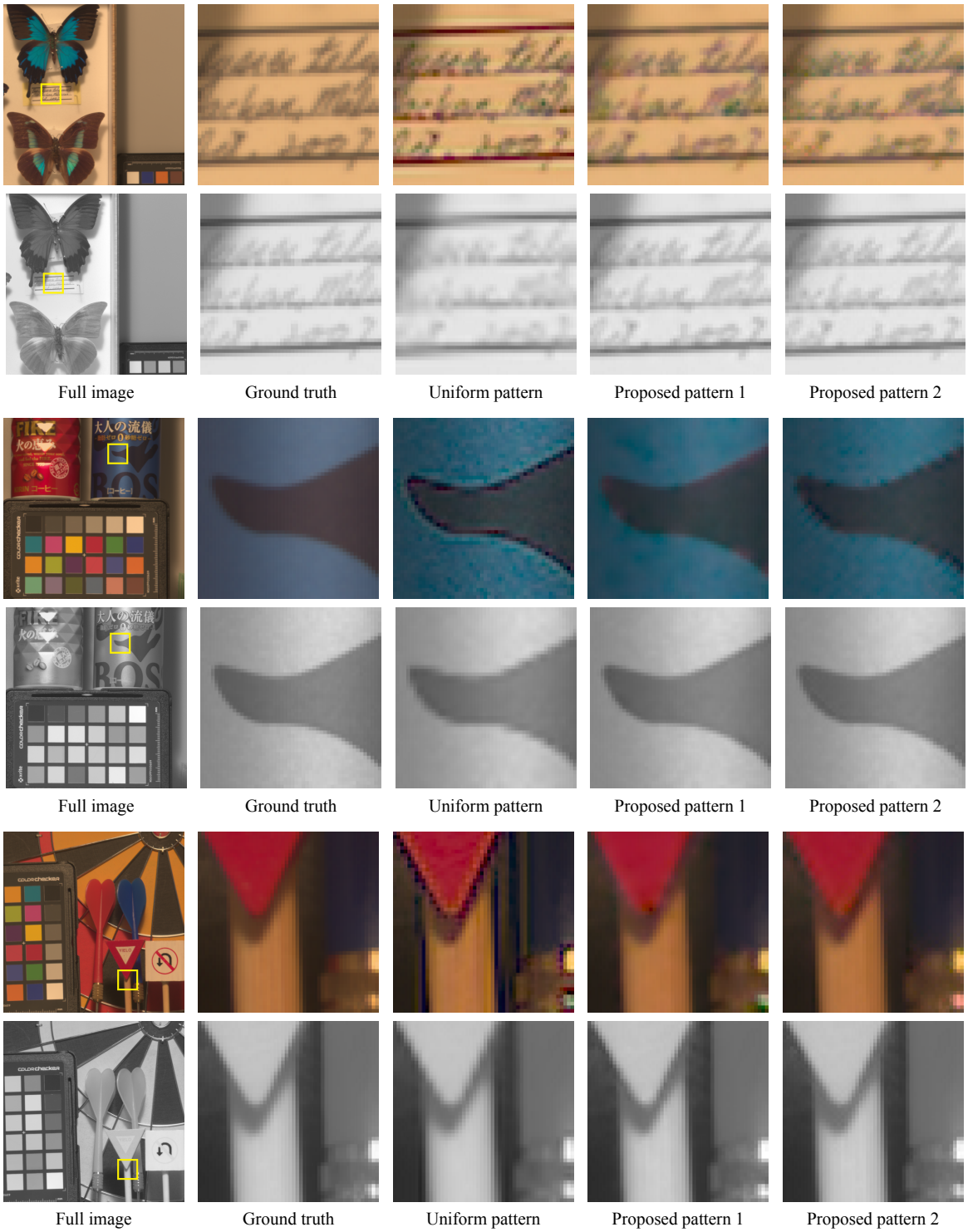

Figure 5: Visual comparison of the acquired RGB and NIR images with different filter array patterns. Left to right: full image, ground truth, uniform RGB-NIR pattern, proposed RGB-NIR pattern 1 and proposed RGB-NIR pattern 2.

DOI: 10.2352/ISSN.2470-1173.2016.18.DPMI-256

vol. 9404, pp. 94040G–1–6, 2015.

[3] D. Connah, M. S. Drew, and G. D. Finlayson, "Spectral edge image fusion: Theory and applications," *Proc. of European Conf. on Computer Vision (ECCV)*, pp. 65–80, 2014.

[4] T. Shibata, M. Tanaka, and M. Okutomi, "Unified image fusion based on application-adaptive importance measure," *Proc. of IEEE Int. Conf. on Image Processing (ICIP)*, 2015.

[5] L. Schaul, C. Fredembach, and S. Süsstrunk, "Color image dehazing using the near-infrared," *Proc. of IEEE Int. Conf. on Image Processing (ICIP)*, pp. 1629–1632, 2009.

[6] C. Feng, S. Zhuo, X. Zhang, L. Shen, and S. Süsstrunk, "Near-infrared guided color image dehazing," *Proc. of IEEE Int. Conf. on Image Processing (ICIP)*, pp. 2363–2367, 2013.

[7] Q. Yan, X. Shen, L. Xu, S. Zhao, X. Zhang, L. Shen, and J. Jia, "Cross-field joint image restoration via scale map," *Proc. of IEEE Int. Conf. on Computer Vision (ICCV)*, pp. 1537–1544, 2013.

[8] H. Honda, R. Timofte, and L. Van Gool., "Make my day - high-fidelity color denoising with near-infrared," *IEEE Workshop on Perception Beyond the Visible Spectrum (PBVS)*, pp. 82–90, 2015.

[9] C. Fredembach D. Rüfenacht and S. Süsstrunk, "Automatic and accurate shadow detection using near-infrared information," *IEEE Trans. on Pattern Analysis and Machine Intelligence*, vol. 36, no. 8, pp. 1672–1678, 2014.

[10] B. Bayer, "Color imaging array," *U.S. Patent 3971065*, 1976.

[11] R. Lukac, *Single-sensor imaging: methods and applications for digital cameras*, CRC Press, 2008.

[12] Y. M. Lu, C. Fredembach, M. Vetterli, and S. Süsstrunk, "Designing color filter arrays for the joint capture of visible and near-infrared images," *Proc. of IEEE Int. Conf. on Image Processing (ICIP)*, pp. 3797–3800, 2009.

[13] Z. Sadeghipoor, Y. M. Lu, and S. Süsstrunk, "Correlation-based joint acquisition and demosaicing of visible and near-infrared images," *Proc. of IEEE Int. Conf. on Image Processing (ICIP)*, pp. 3226–3229, 2011.

[14] K. Kidono and Y. Ninomiya, "Visibility estimation under night-time conditions using a multiband camera," *Proc. of IEEE Intelligent Vehicles Symposium (IV)*, pp. 1013–1018, 2007.

[15] S. Koyama, Y. Inaba, M. Kasano, and T. Murata, "A day and night vision mos imager with robust photonic-crystal-based RGB-and-IR," *IEEE Trans. on Electron Devices*, vol. 55, no. 3, 2008.

[16] Z. Chen, X. Wang, and R. Liang, "RGB-NIR multispectral camera," *Optics Express*, vol. 22, no. 5, pp. 4985–4994, 2014.

[17] H. Tang, X. Zhang, S. Zhuo, F. Chen, K. N. Kutulakos, and L. Shen, "High resolution photography with an RGB-infrared camera," *Proc. of IEEE Int. Conf. on Computational Photography (ICCP)*, 2015.

[18] M. Martinello, A. Wajs, S. Quan, H. Lee, C. Lim, T. Woo, W. Lee, S. S. Kim, and D. Lee, "Dual aperture photography: Image and depth from a mobile camera," *Proc. of IEEE Int. Conf. on Computational Photography (ICCP)*, 2015.

[19] B. K. Gunturk, J. Glotzbach, Y. Altunbasak, R. W. Schafer, and R. M. Mersereau, "Demosaicking: color filter array interpolation," *IEEE Signal Processing Magazine*, vol. 22, pp. 44–54, 2005.

[20] X. Li, B. Gunturk, and L. Zhang, "Image demosaicing: a systematic survey," *Proc. of SPIE*, vol. 6822, pp. 68221J–1–15, 2008.

[21] Y. Monno, M. Tanaka, and M. Okutomi, "N-to-sRGB mapping for single-sensor multispectral imaging," *Proc. of Color and Photometry in Computer Vision Workshop (CPCV)*, 2015.

[22] D. Kiku, Y. Monno, M. Tanaka, and M. Okutomi, "Residual interpolation for color image demosaicking," *Proc. of IEEE Int. Conf. on Image Processing (ICIP)*, pp. 2304–2308, 2013.

[23] D. Kiku, Y. Monno, M. Tanaka, and M. Okutomi, "Simultaneous capturing of RGB and additional band images using hybrid color filter array," *Proc. of SPIE*, vol. 9023, pp. 90230V–1–9, 2014.

[24] Y. Monno, D. Kiku, S. Kikuchi, M. Tanaka, and M. Okutomi, "Multispectral demosaicking with novel guide image generation and residual interpolation," *Proc. of IEEE Int. Conf. on Image Processing (ICIP)*, pp. 645–649, 2014.

[25] J. Y. Hardeberg, F. Schmitt, and H. Brettel, "Multispectral color image capture using a liquid crystal tunable filter," *Optical Engineering*, vol. 41, pp. 2532–2548, 2002.

Author Biography

Hayato Teranaka *received the bachelor degree in control engineering from Tokyo Institute of Technology, Tokyo, Japan, in 2014. He is currently a master student at the Department of Mathematical and Control Engineering at the university. His research interests include image processing and computer vision.*

Yusuke Monno *received the B.E., M.E., and Ph.D degrees from Tokyo Institute of Technology, Tokyo, Japan, in 2010, 2011, and 2014 respectively. He is currently a postdoctoral researcher at the university. From Nov. 2013 to Mar. 2014, he joined the Image and Visual Representation Group at Ecole Polytechnique Federale de Lausanne, Switzerland, as a research internship student. His research interests are in both theoretical and practical aspects of computer vision and image processing. He is a member of IEEE.*

Masayuki Tanaka *received his bachelor and master degrees in control engineering and Ph.D. degree from Tokyo Institute of Technology in 1998, 2000, and 2003. He joined Agilent Technology in 2003. He was a Research Scientist at Tokyo Institute of Technology since 2004 to 2008. Since 2008, He has been an Associated Professor at the Graduate School of Science and Engineering, Tokyo Institute of Technology. He was a Visiting Scholar with Department of Psychology, Stanford University, CA, USA.*

Masatoshi Okutomi *received the B.Eng. degree from the Department of Mathematical Engineering and Information Physics, University of Tokyo, Tokyo, Japan, in 1981, and the M.Eng. degree from the Department of Control Engineering, Tokyo Institute of Technology, Tokyo, in 1983. He joined the Canon Research Center, Canon Inc., Tokyo, in 1983. From 1987 to 1990, he was a Visiting Research Scientist with the School of Computer Science, Carnegie Mellon University, Pittsburgh, PA, USA. He received the Dr.Eng. degree from the Tokyo Institute of Technology, in 1993, for his research on stereo vision. Since 1994, he has been with the Tokyo Institute of Technology, where he is currently a Professor with the Department of Mechanical and Control Engineering, Graduate School of Science and Engineering.*